IEEE Photonics Journal
An IEEE Photonics Society Publication

Open Access

Trapping Two Types of Particles Using a Laguerre–Gaussian Correlated Schell-Model Beam

Volume 8, Number 5, October 2016

Yuan Zhou
Hua-Feng Xu
Yangsheng Yuan
Ji Peng
Jun Qu
Wei Huang

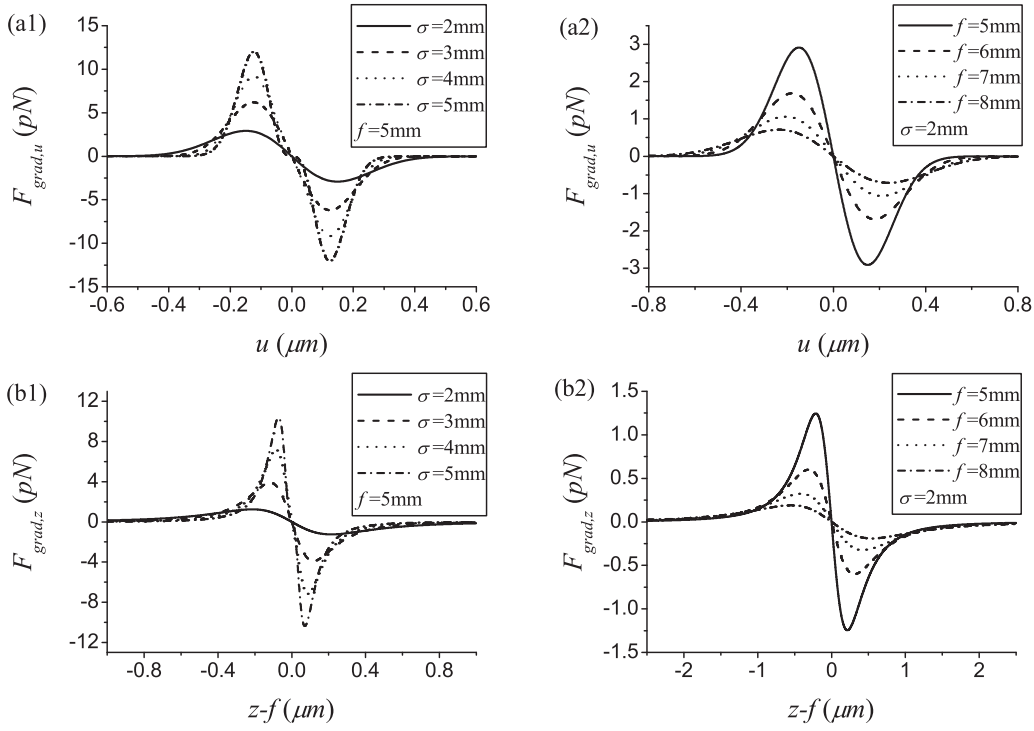

DOI: 10.1109/JPHOT.2016.2613741
1943-0655 © 2016 IEEE

Trapping Two Types of Particles Using a Laguerre–Gaussian Correlated Schell-Model Beam

Yuan Zhou,[1] Hua-Feng Xu,[2,3] Yangsheng Yuan,[1] Ji Peng,[4] Jun Qu,[1] and Wei Huang[2,3]

[1]Department of Physics and Electronic Information, Anhui Normal University, Wuhu, Anhui 241000, China
[2]Laboratory of Atmospheric Physico-Chemistry, Anhui Institute of Optics and Fine Mechanics, Chinese Academy of Sciences, Hefei, Anhui 230031, China
[3]School of Environmental Science and Optoelectronic Technology, University of Science and Technology of China, Hefei, Anhui 230026, China
[4]National Engineering Laboratory of Special Display Technology, Wuhu 241000, China

DOI:10.1109/JPHOT.2016.2613741

Manuscript received August 16, 2016; revised September 20, 2016; accepted September 22, 2016. Date of publication September 26, 2016; date of current version October 13, 2016. This work was supported in part by the National Natural Science Foundation of China (NSFC) under Grant 11374015 and Grant 21133008 and in part by the Anhui Provincial Natural Science Foundation under Grant 1408085MKL87. Corresponding authors: J. Qu and W. Huang (e-mail: qujun70@mail.ahnu.edu.cn; huangwei6@ustc.edu.cn).

Abstract: Based on the Rayleigh scattering theory, the radiation forces and the trap stiffness on Rayleigh dielectric sphere induced by a focused Laguerre–Gaussian correlated Schell-model (LGCSM) beam are theoretically studied. It is found that by choosing the appropriate transverse coherence width, mode orders, transverse beam width, and focus lengths, a Rayleigh particle whose refractive index is larger or smaller than the ambient medium can be trapped. Our results will have some theoretical reference value for optical trapping.

Index Terms: Laguerre-Gaussian correlated Schell-model beam (LGCSM), radiation forces, trap stiffness.

1. Introduction

Since Gori *et al.* established the sufficient condition for devising a genuine correlation function of a scalar or electromagnetic partially coherent beam [1]–[3], increasingly more attention is being paid to partially coherent beams with nonconventional correlation functions. A variety of partially coherent beams with nonconventional correlation functions has been proposed and studied both theoretically and experimentally in recent years, such as the nonuniformly correlated Gaussian Schell-model beam [4]–[7], the multi-Gaussian correlated Schell-model beam [8]–[12], the cosine-Gaussian correlated Schell-model beam [13]–[15], the special correlated partially coherent vector beam [16], the Bessel-Gaussian correlated Schell-model beam [17], [18], and the Hermite-Gaussian correlated Schell-model beam [19]. It was found that those partially coherent beams exhibit some extraordinary propagation properties, such as far field flat-topped beam profile formation [8], [9], far field ring-shaped beam profile formation [13], [17], self-focusing effect [6], self-splitting effect [19], and lateral shift of the intensity maximum [5], [6].

Optical trapping and manipulation have become a hot topic in scientific community since the pioneering work of Ashkin [20]. Now, optical trapping has been widely applied in physics, chemistry,

and biophysical studies, for example, the manipulation of micronized dielectric particles, neutral atoms, DNA molecules, and living biological cells [21]–[28]. It is known that by using different type of laser beams, the effective and stable trapping of particles with different refractive indices can be implemented. For example, the particles with refractive index larger than the ambient medium can be trapped by flat-topped beams [21], GSM beams [29], or Lorentz-Gauss beams [30]. On the other hand, the particles with refractive index smaller than the ambient medium can be trapped by dark hollow beams [32]. Meanwhile, it is shown that one can trap two types of particles with different refractive indices using bottle beams [31], partially coherent elegant Laguerre-Gaussian beams [32] or elegant Hermite-cosine-Gaussian beams [33]. Thus, it is significant to study the optical trapping properties of different types of laser beams.

On the other hand, the study on the optical trapping properties of partially coherent beams is always a subject of great interest due to its practical applications in optical trapping [21], [29], [32], [34]–[36]. Recently, the optical trapping properties of several partially coherent beams with nonconventional correlation functions, such as the multi-Gaussian correlated Schell-model beam, the cosine-Gaussian correlated Schell-model beam, and the generalized Multi-Gaussian Schell-model beam have been studied [34]–[36]. All of these beams can trap two types of Rayleigh particles with different refractive indices, but each beam has its distinctive feature. Recently, the Laguerre-Gaussian correlated Schell-model (LGCSM) beam was proposed theoretically [17] and generated experimentally [37]. It was found that the intensity distribution of LGCSM beam displays a Gaussian profile at the source plane, while the far-field intensity distribution exhibits a ring-shaped profile [37], [39], [42], [45], [46]. Due to their significant application in optical trapping and free-space optical communications, LGCSM beam have attracted a great deal of attention [37]–[48]. As far as we known, the trapping properties of LGCSM beams have not yet been reported. Thus, it is of significance to study the optical trapping properties of LGCSM beam.

In this paper, we have derived the analytical formulas for the beam intensity distribution of a focused LGCSM beam through an ABCD optical system. Based on the Rayleigh scattering theory, the radiation forces and trap stiffness on Rayleigh dielectric sphere induced by a focused LGCSM beam are theoretically studied. It is found that by changing the transverse coherence width, two types of particles with different refractive index can be trapped stably by a focused LGCSM beam. Our results will have some theoretical reference value for optical trapping.

2. Analytical Formulas for the Beam Intensity Distribution of a Focused LGCSM Beam

In the Cartesian coordinate system, the cross-spectral density function of the LGCSM beam at the source plane ($z = 0$) can be expressed as [17]

$$W(\mathbf{r}_1, \mathbf{r}_2, 0) = I_0 \exp\left(-\frac{|\mathbf{r}_1|^2 + |\mathbf{r}_2|^2}{4\sigma^2} - \frac{|\mathbf{r}_1 - \mathbf{r}_2|^2}{2\delta^2}\right) L_n\left(\frac{|\mathbf{r}_1 - \mathbf{r}_2|^2}{2\delta^2}\right) \tag{1}$$

where I_0 is a constant, $\mathbf{r}_1 = (x_1, y_1)$ and $\mathbf{r}_2 = (x_2, y_2)$ are two arbitrary position vector at the source plane, σ and δ denote the transverse beam width and the transverse coherence width, and L_n is Laguerre polynomial of mode orders n.

According to Collins formula, the propagation of the cross-spectral density function of the LGCSM beam through an $ABCD$ optical system can be expressed as [47]

$$\begin{aligned} W(u_1, u_2, v_1, v_2, z) = {} & \frac{1}{\lambda^2 B^2} \int_{-\infty}^{\infty}\int_{-\infty}^{\infty}\int_{-\infty}^{\infty}\int_{-\infty}^{\infty} W(x_1, x_2, y_1, y_2, 0)\, dx_1 dx_2 dy_1 dy_2 \\ & \times \exp\left[-\frac{ik}{2B}\left(A x_1^2 - 2x_1 u_1 + D u_1^2\right) - \frac{ik}{2B}\left(A y_1^2 - 2y_1 v_1 + D v_1^2\right)\right] \\ & \times \exp\left[\frac{ik}{2B}\left(A x_2^2 - 2x_2 u_2 + D u_2^2\right) + \frac{ik}{2B}\left(A y_2^2 - 2y_2 v_2 + D v_2^2\right)\right] \end{aligned} \tag{2}$$

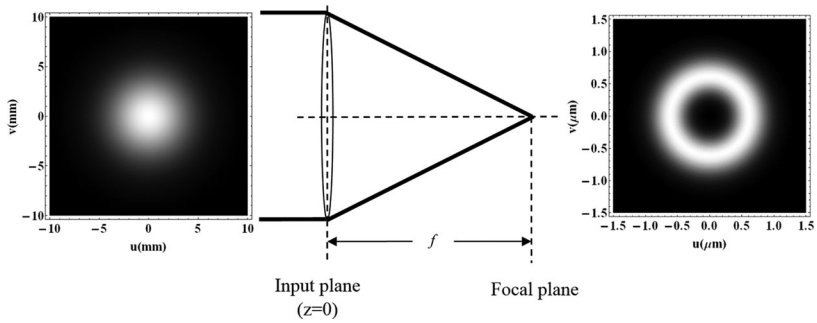

Fig. 1. Scheme of the optical system. Plots of the left and right are the intensity distribution of the LGCSM beam at the input and focal planes.

Where x_i and y_i and u_i and v_i denote the coordinate at the input plane and the output plane, and $k = 2\pi/\lambda$ represents the wave number with the wavelength λ. Besides, A, B, C, and D indicate the elements of a transfer matrix for the optical system (see Fig. 1) and can be expressed as

$$\begin{pmatrix} A & B \\ C & D \end{pmatrix} = \begin{pmatrix} 1 - \frac{z}{f} & z \\ -\frac{z}{f} & 1 \end{pmatrix}. \tag{3}$$

For the convenience of integration, we consider $u_1 = u_2 = u$, $v_1 = v_2 = v$. We assumed that the power of LGCSM beam is P. Substituting (1) and (3) into (2), the analytical formulas for the beam intensity of a focused LGCSM beam are theoretically derived through complex operation as follows:

$$\begin{aligned}
&I_{\text{out}}(u, v, z) = W(u, v, z) \\
&= I_0 \frac{\pi^2}{\lambda^2 B^2 F_1} \sum_{g=0}^{n} \sum_{h=0}^{2g} \sum_{j=0}^{2n-2g} \sum_{l=0}^{2g-h} \sum_{m=0}^{2n-2g-j} \sum_{s=0}^{\left[\frac{h}{2}\right]} \sum_{t=0}^{\left[\frac{2g-h-l}{2}\right]} \sum_{p=0}^{\left[\frac{j}{2}\right]} \sum_{q=0}^{\left[\frac{2n-2g-j-m}{2}\right]} (-1)^{h-s+j-p+n+t+q} \\
&\times 2^{-\frac{2g-h+2n-2g-j}{2}} i^{-3n-h+2s-2g+h+l+2t+2p-2n+2g+m+2q} \delta^{2s+h+2l+4t+2p-4n+j+2m+4q} \\
&\times F_2^{h+l+2t-2n+j+m+2q} F_3^{-\frac{-2s-l-2t-2p+2n-m-2q+2}{2}} \left(1 - \frac{1}{F_1 \delta^2}\right)^{\frac{2g-h+2n-2g-j}{2}} \binom{n}{g} \binom{2g}{h} \binom{2n-2g}{j} \\
&\times \binom{2g-h}{l} \binom{2n-2g-j}{m} \frac{1}{n!} \frac{h!}{s!\,(h-2s)!} \frac{j!}{p!\,(j-2p)!} \frac{(2g-h-l)!}{t!\,(2g-h-l-2t)!} \frac{(2n-2g-j-m)!}{q!\,(2n-2g-j-m-2q)!} \\
&\times \exp\left[\left(-\frac{k^2}{4F_1 B^2} + \frac{F_4^2}{4F_3}\right)(u^2 + v^2)\right] H_l\left(\frac{iku}{BF_2}\right) H_m\left(\frac{ikv}{BF_2}\right) \\
&\times H_{h-2s+2g-h-l-2t}\left(\frac{iF_4 u}{2\sqrt{F_3}}\right) H_{j-2p+2n-2g-j-m-2q}\left(\frac{iF_4 v}{2\sqrt{F_3}}\right)
\end{aligned} \tag{4}$$

where

$$\begin{aligned}
I_0 &= \frac{P}{2\sigma^2 \pi} \\
F_1 &= \frac{1}{4\sigma^2} + \frac{1}{2\delta^2} + \frac{ikA}{2B} \\
F_2 &= \sqrt{2}\sqrt{F_1}\sqrt{F_1 \delta^2 - 1}, \\
F_3 &= \frac{1}{4\sigma^2} + \frac{1}{2\delta^2} - \frac{ikA}{2B} - \frac{1}{4F_1 \delta^4} \\
F_4 &= \frac{ik}{2F_1 \delta^2 B} - \frac{ik}{B}.
\end{aligned} \tag{5}$$

The following integral formula has been used in the derivation of the above (4) [49], [50]

$$L_n^m(\rho^2) = \frac{(-1)^n}{2^{2n}n!}\sum_{r=0}^{n}\binom{n}{r}H_{2r}(x)H_{2(n-r)}(y) \tag{6}$$

$$H_n(x+y) = 2^{-\frac{n}{2}}\sum_{k=0}^{n}\binom{n}{k}H_{n-k}\left(\sqrt{2}x\right)H_k\left(\sqrt{2}y\right) \tag{7}$$

$$\int_{-\infty}^{\infty}H_n(\alpha x)\exp\left[-(x-y)^2\right]dx = \sqrt{\pi}\left(1-\alpha^2\right)^{\frac{n}{2}}H_n\left(\frac{\alpha y}{\sqrt{1-\alpha^2}}\right) \tag{8}$$

$$H_n(x) = \sum_{k=0}^{\left[\frac{n}{2}\right]}\frac{(-1)^k n!}{k!(n-2k)!}(2x)^{n-2k} \tag{9}$$

$$\int_{-\infty}^{\infty}x^n\exp\left[-(x-b)^2\right]dx = (2i)^{-n}\sqrt{\pi}H_n(ib). \tag{10}$$

3. Analytical Formulas for the Radiation Force and Trap Stiffness on Rayleigh Dielectric Sphere Induced by a Focused LGCSM Beam

The Rayleigh dielectric sphere can be regarded as an electric dipole while the radius is much smaller than the wavelength (radius of particle: $a \ll \lambda$). The radiation forces on a Rayleigh dielectric sphere induced by a focused LGCSM beam can be investigated by using the Rayleigh scattering theory.

The momentum of the incident light and Rayleigh dielectric sphere has been exchanged on the proceeding of the incident light being scattering by Rayleigh dielectric sphere. The sign of scattering force $\mathbf{F}_{\text{scat}}$ denote the direction of it. The scattering force with positive sign is along the direction of beam propagation ($+z$). According to the Rayleigh scattering theory, the scattering force is expressed as [23]

$$\mathbf{F}_{\text{scat}} = \frac{8\pi n_m k^4 a^6}{3c}\left(\frac{m^2-1}{m^2+2}\right)^2 I_{\text{out}}(u,v,z)\,\mathbf{z} \tag{11}$$

where $I_{\text{out}}(u,v,z)$ is the intensity of the focused LGCSM beam at the output plane, c is the speed of light in a vacuum, $\mathbf{z}$ is a unit vector along the beam propagation, n_m denotes the refractive index of the ambient medium, and $m = n_p/n_m$ with n_p represents the refractive index of Rayleigh dielectric sphere.

Another kind of radiation force that generated by focused LGCSM beam on the Rayleigh dielectric sphere is gradient force. The gradient force is proportional to the gradient of the square of the electric field numerical. The gradient force $\mathbf{F}_{\text{grad},u}$ and $\mathbf{F}_{\text{grad},z}$ with positive sign are along the direction of $+u$ and $+z$. According to the Rayleigh scattering theory, the gradient force is expressed as [23]

$$\mathbf{F}_{\text{grad}} = \frac{2\pi n_m a^3}{c}\frac{m^2-1}{m^2+2}\nabla I_{\text{out}}(u,v,z) \tag{12}$$

Besides, the magnitude of trap stiffness can reflect the trapping stability directly. The transverse and on-axis longitudinal trap stiffness can be expressed as [28], [51]

$$\kappa_t = \left|\frac{\partial \mathbf{F}_t}{\partial u}\right|_{\text{Uequ}}, \kappa_z = \left|\frac{\partial \mathbf{F}_z}{\partial z}\right|_{\text{Zequ}}. \tag{13}$$

where $\mathbf{F}_t = \mathbf{F}_{\text{scat},u} + \mathbf{F}_{\text{grad},u} + \mathbf{F}_{\text{abs},u}$ and $\mathbf{F}_z = \mathbf{F}_{\text{scat},z} + \mathbf{F}_{\text{grad},z} + \mathbf{F}_{\text{abs},z}$ denotes the total trapping force on the transverse or along the axial, $\mathbf{F}_{\text{abs}}$ is the absorption force on Rayleigh dielectric sphere induced by a focused LGCSM beam. Due to the absorption force is much smaller than the gradient force, the total trapping force on the transverse or along the axial can be approximated as $\mathbf{F}_t = \mathbf{F}_{\text{scat},u} + \mathbf{F}_{\text{grad},u}$ and $\mathbf{F}_z = \mathbf{F}_{\text{scat},z} + \mathbf{F}_{\text{grad},z}$.

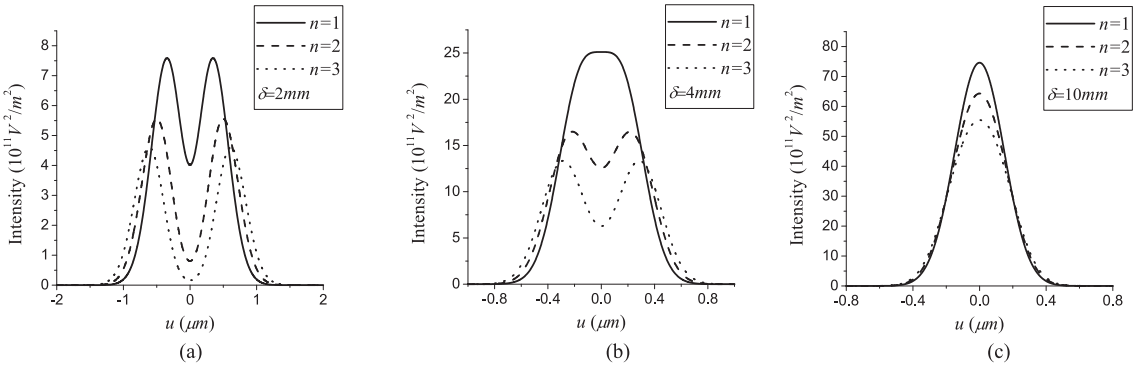

Fig. 2. Intensity distribution of focused LGCSM beams at $z = f$ with different values of transverse coherence width δ and mode order n.

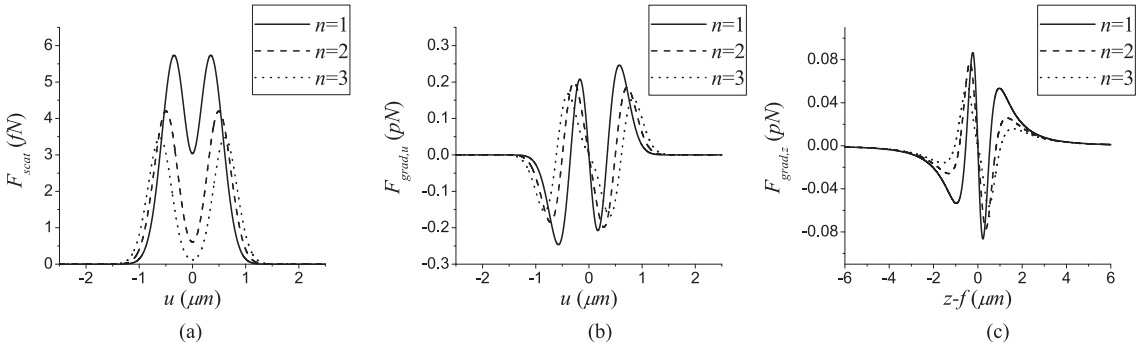

Fig. 3. Scattering force and gradient force of focused LGCSM beam on a Rayleigh particle with different mode order n and $\delta = 2$ mm.

4. Numerical Results and Analysis

According to (4), (11), (12), and (13), we made an analysis about the beam intensity of a focused LGCSM beam and the trapping properties on Rayleigh particles.

In Fig. 2, the calculation parameters are set as $\lambda = 632.8$ nm, $P = 1$ W, $f = 5$ mm, and $\sigma = 2$ mm (The beam power $P = 1$ W is simply examples). It is found that the profile of a focused LGCSM beam can be shaped by changing the transverse coherence width δ, For a smaller δ, the focused LGCSM beam exhibits a ring-shaped beam profile, and the focused LGCSM beam converts to Gaussian beam profile with the increase of δ. Meanwhile, the peak value of the intensity decreases with the increase of n. Thus, one can shape the profile of a focused LGCSM beam by choosing an appropriate coherence width, which will be useful for trapping different types of Rayleigh particles using a focused LGCSM beam.

In Fig. 3, the calculation parameters are set as $a = 30$ nm, $n_m = 1.33$, and $n_p = 1$, other parameters are the same as in Fig. 2, in which we calculate the scattering force (see Fig. 3(a)) and transverse gradient force (see Fig. 3(b)) at the focal plane (crossline $v = 0$), and the on-axis longitudinal gradient force (see Fig. 3(c)) of a focused LGCSM beam on a Rayleigh particle. From Fig. 3(b) and 3(c), one can see that there is a stable equilibrium point at the focus, so the Rayleigh particle whose refractive index is smaller than the ambient medium can be trapped by a focused LGCSM beam with small transverse coherence width δ. Besides, the transverse and longitudinal trapping range increases with the increase of mode order n. Thus, by choose suitable transverse coherence width and mode order, one can use a focused LGCSM beam to trap a Rayleigh particle whose refractive index is smaller than the ambient medium.

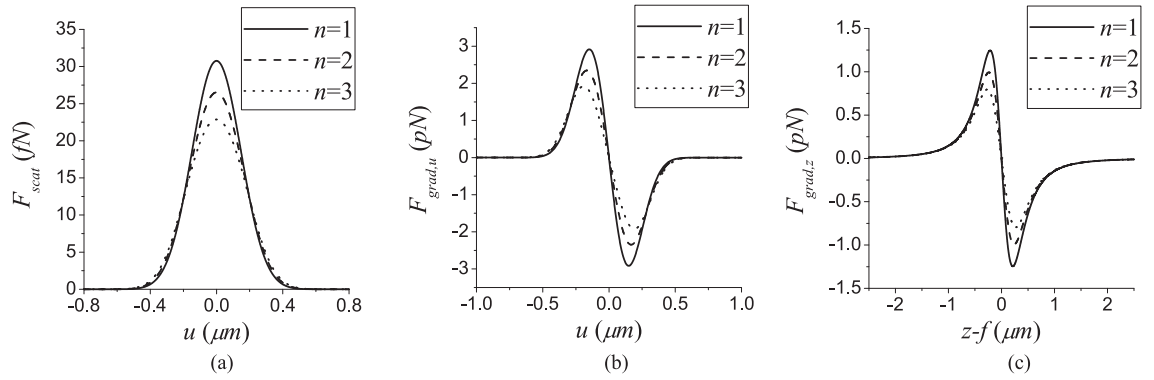

Fig. 4. Scattering force and gradient force of focused LGCSM beam on a Rayleigh particle with different mode order n and $\delta = 10$ mm.

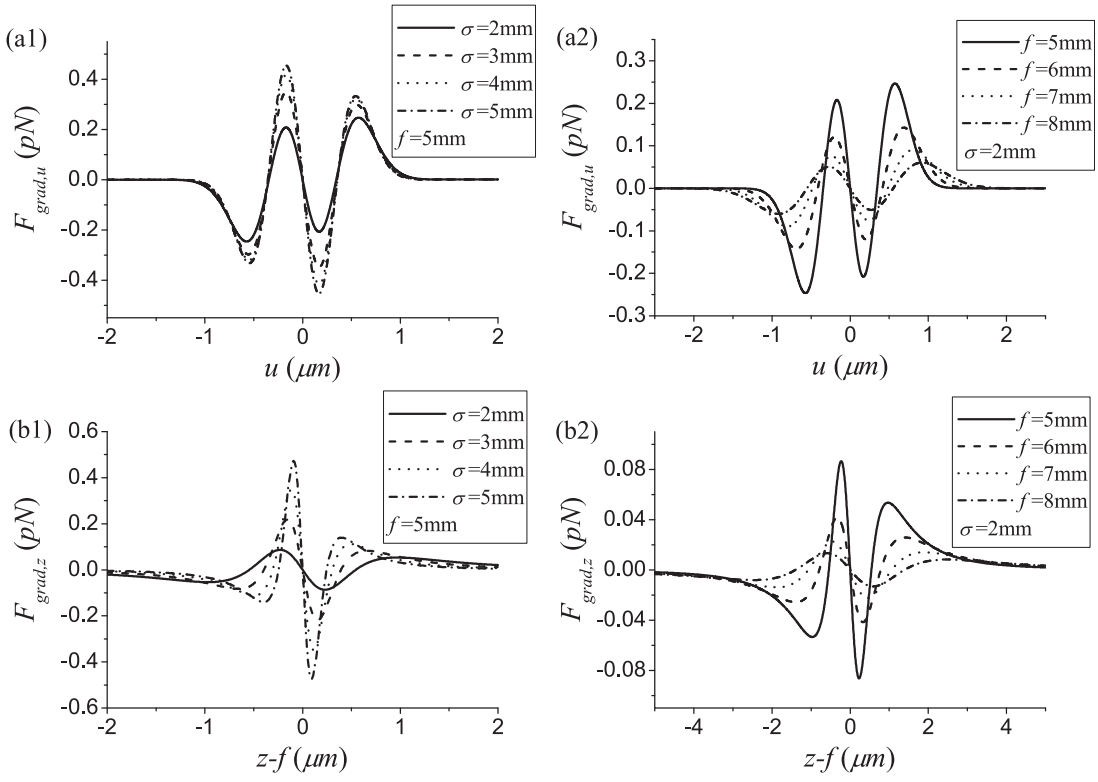

Fig. 5. Transverse gradient force and on-axis longitudinal gradient force at the focal plane of focused LGCSM beam on a Rayleigh particle with different value of σ and f ($\delta = 2$ mm).

In Fig. 4, the calculation parameters are set as $a = 30$ nm, $n_m = 1.33$, and $n_p = 1.59$; other parameters are the same as in Fig. 2. In Fig. 2, we calculate the scattering force (see Fig. 4(a)) and transverse gradient force (see Fig. 4(b)) at the focal plane (crossline $v = 0$), and the on-axis longitudinal gradient force (see Fig. 4(c)) of a focused LGCSM beam on a Rayleigh particle. From Fig. 4(b) and 4(c), one can see that there is a stable equilibrium point at the focus, so the Rayleigh particle whose refractive index is larger than the ambient medium can be trapped by a focused LGCSM beam with large transverse coherence width δ. Thus, by choose suitable transverse coherence width and mode order, one can use a focused LGCSM beam to trap a Rayleigh particle whose refractive index is larger than the ambient medium.

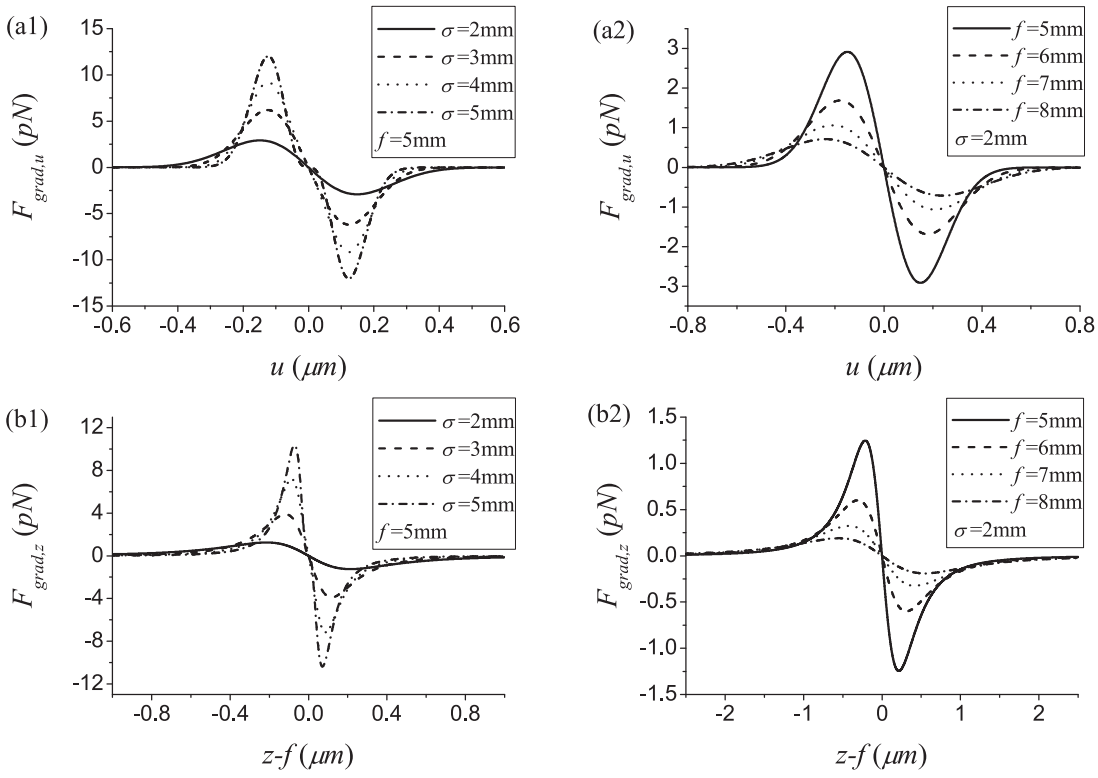

Fig. 6. Transverse gradient force and on-axis longitudinal gradient force at the focal plane of focused LGCSM beam on a Rayleigh particle with different value of σ and f ($\delta = 10$ mm).

Based on the Rayleigh scattering theory, the gradient force should be able to overcome the scattering force and the Brownian motion [32]. From Figs. 3 and 4, one can see that the gradient force are much larger than the scattering force. According to the fluctuation-dissipation theorem of Einstein, the magnitude of the Brownian force is $F_B = 2.5$ fN (for water at $T = 300$ K) [32]. One can see that the gradient force is larger than the Brownian force. Thus, the particles can be trapped stably by a focused LGCSM beam. Besides, the transverse gradient force and longitudinal gradient force decreases with the increase of mode order. Therefore, one can choose a smaller mode order in order to trapping a particle stably.

In Fig. 5, the parameters are set as $n = 1$, $\delta = 2$ mm, $a = 30$ nm, $n_m = 1.33$, and $n_p = 1$, and other parameters are the same as in Fig. 2. From Fig. 5(a1) and 5(b1), one can see that the transverse gradient force and the longitudinal gradient force increases with the increase of transverse beam width. However, the longitudinal trapping ranger is decreasing at the same time. From Fig. 5(a2) and 5(b2), one can see that the transverse gradient force and longitudinal gradient force decreases with the increases of focal length f. In the same time, the trapping range is increasing both in transverse and in longitudinal. Thus, one can use a focused LGCSM with a small transverse coherence width δ to trap a Rayleigh particle whose refractive index is smaller than the ambient medium.

In Fig. 6, the parameters are set as $n = 1$, $\delta = 10$ mm, $a = 30$ nm, $n_m = 1.33$, and $n_p = 1.59$, and other parameters are the same as in Fig. 2. From Fig. 6(a1) and 6(b1), one can see that the transverse gradient force and longitudinal gradient force increases with the increase of transverse beam width, and the longitudinal trapping range is decreasing at the same time. As is shown in Fig. 6(a2) and 6(b2), the transverse gradient force and the longitudinal gradient force decreases with the increases of focal length. Meanwhile, the longitudinal trapping ranger increases. Thus, one can use a focused LGCSM with a large transverse coherence width δ to trap a Rayleigh particle whose refractive index is smaller than the ambient medium.

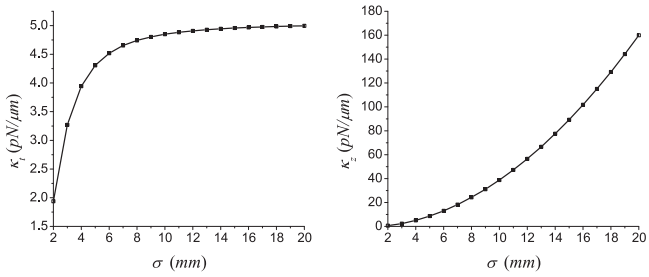

Fig. 7. Dependence of the transverse and on-axis longitudinal trap stiffness on the transverse beam width σ at the focus point ($\delta = 2$ mm).

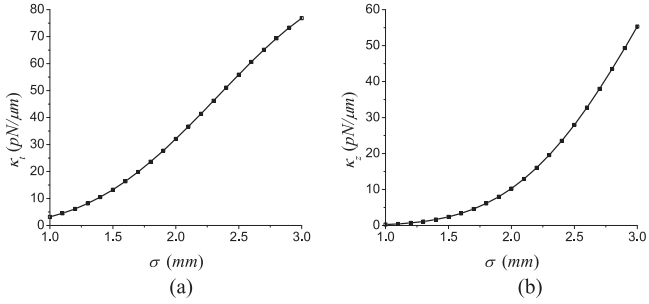

Fig. 8. Dependence of the transverse and on-axis longitudinal trap stiffness on the transverse beam width σ at the focus point ($\delta = 10$ mm).

From Fig. 5 and 6, one can find that by choosing suitable transverse beam width and focal length, one can trap particles with a larger range and better stability.

Figs. 7 and 8 shows the dependence of the transverse trap stiffness (see Figs. 7(a) and 8(a)) and on-axis longitudinal trap stiffness (see Figs. 7(b) and 8(b)) on the transverse beam width at the focus point. The parameters in Fig. 7 are the same as in Fig. 3. Besides, the focused beam intensity of LGCSM beam in Fig. 7 has a ring-shaped beam profile while 2 mm $\leq \sigma \leq$ 20 mm. Fig. 8, the parameters are the same as in Fig. 4, and the focused beam intensity of LGCSM beam in Fig. 8 will keep Gaussian beam profile while 1 mm $\leq \sigma \leq$ 3 mm. One can find from Fig. 7 that the transverse and on-axis longitudinal trap stiffness both increases with the increase of transverse beam width σ. From Fig. 8, one can find that the transverse and on-axis longitudinal trap stiffness both increases with the increase of transverse beam width σ. From these two figures, one can find that by choosing suitable mode order and transverse beam width, two types of Rayleigh particles can be trapped stably.

5. Conclusions

In this paper, the beam intensity distribution, radiation force, and trap stiffness on the Rayleigh dielectric sphere of a focused LGCSM beam are theoretically studied. It is found that the beam profile of a focused LGCSM beam can be shaped by changing the transverse coherence width. So one can trap two types of Rayleigh dielectric sphere with different refractive index using a focused LGCSM beam. With a small transverse coherence width, the focused LGCSM beam has a ring-shaped beam profile, and the focused LGCSM beam convert to Gaussian beam profile with the increase of coherence width. Meanwhile, the peak value of the intensity decreases with the increase of mode order. By choosing a suitable mode order, not only can the trapping stability can be enhanced, but the trapping range can be enlarged as well. While the mode order is given, one

can choose a suitable transverse beam width and focal length to enhance the trapping stability and enlarge the trapping range. Thus, by changing the transverse coherence width and choose suitable mode order, transverse beam width and focal length of a focused LGCSM beam, two different types of Rayleigh particles can be trapped stably in a large range.

References

[1] F. Gori and M. Santarsiero, "Devising genuine spatial correlation functions," *Opt. Lett.*, vol. 32, no. 24, pp. 3531–3533, Dec. 2007.

[2] F. Gori, V. Ramrez Sanchez, M. Santarsiero, and T. Shirai, "On genuine cross-spectral density matrices," *J. Opt. A: Pure Appl. Opt.*, vol. 11, no. 8, May 2009, Art. no. 085706.

[3] R. Martnez Herrero, P. M. Mejas, and F. Gori, "Genuine cross-spectral densities and pseudo-modal expansions," *Opt. Lett.*, vol. 34, no. 9, pp. 1399–1401, May 2009.

[4] H. Lajunen and T. Saastamoinen, "Propagation characteristics of partially coherent beams with spatially varying correlations," *Opt. Lett.*, vol. 36, no. 20, pp. 4104–4106, Oct. 2011.

[5] Z. Tong and O. Korotkova, "Nonuniformly correlated light beams in uniformly correlated media," *Opt. Lett.*, vol. 37, no. 15, pp. 3240–3242, Aug. 2012.

[6] Z. Tong and O. Korotkova, "Electromagnetic nonuniformly correlated beams," *J. Opt. Soc. Amer. A*, vol. 29, no. 10, pp. 2154–2158, Oct. 2012.

[7] Y. Gu and G. Gbur, "Scintillation of nonuniformly correlated beams in atmospheric turbulence," *Opt. Lett.*, vol. 38, no. 9, pp. 1395–1397, May 2013.

[8] O. Korotkova, S. Sahin, and E. Shchepakina, "Multi-Gaussian Schell-model beams," *J. Opt. Soc. Amer. A*, vol. 29, no. 10, pp. 2159–2164, Oct. 2012.

[9] Y. Zhang, L. Liu, C. Zhao, and Y. Cai, "Multi-Gaussian Schell-model vortex beam," *Phys. Lett. A*, vol. 378, no. 9, pp. 750–754, Jan. 2014.

[10] O. Korotkova and E. Shchepakina, "Rectangular Multi-Gaussian Schell-Model beams in atmospheric turbulence," *J. Opt.*, vol. 16, no. 4, Mar. 2014, Art. no. 045704.

[11] Y. Yuan *et al.*, "Scintillation index of a multi-Gaussian Schell-model beam in turbulent atmosphere," *Opt. Commun.*, vol. 305, no. 3, pp. 57–65, Sep. 2013.

[12] Z. Mei, O. Korotkova, and E. Shchepakina, "Electromagnetic multi-Gaussian Schell-model beams," *J. Opt.*, vol. 15, no. 2, Dec. 2012, Art. no. 025705.

[13] Z. Mei and O. Korotkova, "Cosine-Gaussian Schell-model sources," *Opt. Lett.*, vol. 38, no. 14, pp. 2578–2580, Jul. 2013.

[14] C. Liang, F. Wang, X. Liu, Y. Cai, and O. Korotkova, "Experimental generation of cosine-Gaussian–correlated Schell-model beams with rectangular symmetry," *Opt. Lett.*, vol. 39, no. 4, pp. 769–772, Feb. 2014.

[15] Z. Mei, E. Shchepakina, and O. Korotkova, "Propagation of cosine-Gaussian–correlated Schell-model beams in atmospheric turbulence," *Opt. Exp.*, vol. 21, no. 15, pp. 17512–17519, Jul. 2013.

[16] Y. Chen, F. Wang, L. Liu, C. Zhao, Y. Cai, and O. Korotkova, "Generation and propagation of a partially coherent vector beam with special correlation functions," *Phys. Rev. A*, vol. 89, no. 1, Jan. 2014, Art. no. 013801.

[17] Z. Mei and O. Korotkova, "Random sources generating ring–shaped beams," *Opt. Lett.*, vol. 38, no. 2, pp. 91–93, Jan. 2013.

[18] Y. Cai, Y. Chen, and F. Wang, "Generation and propagation of partially coherent beams with nonconventional correlation functions: A review," *J. Opt. Soc. Amer. A*, vol. 31, no. 9, pp. 2083–2096, Sep. 2014.

[19] Y. Chen, J. Gu, F. Wang, and Y. Cai, "Self-splitting properties of a Hermite-Gaussian correlated Schell-model beam," *Phys. Rev. A*, vol. 91, no. 1, Jan. 2015, Art. no. 013823.

[20] A. Ashkin, "Acceleration and trapping of particles by radiation pressure," *Phys. Rev. Lett.*, vol. 24, no. 4, pp. 156–159, Jan. 1970.

[21] C. Zhao, Y. Cai, X. Lu, and H. T. Eyyubolu, "Radiation force of coherent and partially coherent flat–topped beams on a Rayleigh particle," *Opt. Exp.*, vol. 17, no. 3, pp. 1753–1765, Feb. 2009.

[22] D. Zhang, X. C. Yuan, S. C. Tjin, and S. Krishnan, "Rigorous time domain simulation of momentum transfer between light and microscopic particles in optical trapping," *Opt. Exp.*, vol. 12, no. 10, pp. 2220–2230, May 2004.

[23] Y. Harada and T. Asakura, " Radiation forces on a dielectric sphere in the Rayleigh scattering regime," *Opt. Commun.*, vol. 124, no. 5, pp. 529–541, Mar. 1996.

[24] S. M. Block, L. S. Goldstein, and B. J. Schnapp, "Bead movement by single kinesin molecules studied with optical tweezers," *Nature*, vol. 348, no. 6229, pp. 348–352, Nov. 1990.

[25] L. Oroszi, P. Galajda, H. Kirei, S. Bottka, and P. Ormos, "Direct measurement of torque in an optical trap and its application to double-strand DNA," *Phys. Rev. Lett.*, vol. 97, no. 5, Aug. 2006, Art. no. 058301.

[26] C. Day, "Optical trap resolves the stepwise transfer of genetic information from DNA to RNA," *Phys. Today*, vol. 59, no. 1, pp. 26–27, Jan. 2006.

[27] A. A. Ambardekar and Y. Li, "Optical levitation and manipulation of stuck particles with pulsed optical tweezers," *Opt. Lett.*, vol. 30, no. 14, pp. 1797–1799, Jul. 2005.

[28] Q. Zhan, "Trapping metallic Rayleigh particles with radial polarization," *Opt. Exp.*, vol. 12, no. 15, pp. 3377–3382, Jul. 2004.

[29] L. Wang, C. Zhao, L. Wang, X. Lu, and S. Zhu, "Effect of spatial coherence on radiation forces acting on a Rayleigh dielectric sphere," *Opt. Lett.*, vol. 32, no. 11, pp. 1393–1395, Jun. 2007.

[30] Y. Jiang, K. Huang, and X. Lu, "Radiation force of highly focused Lorentz–Gauss beams on a Rayleigh particle," *Opt. Exp.*, vol. 19, no. 10, pp. 9708–9713, May 2011.

[31] C. H. Chen, P. T. Tai, and W. F. Hsieh, "Bottle beam from a bare laser for single-beam trapping," *Appl. Opt.*, vol. 43, no. 32, pp. 6001–6006, Nov. 2004.
[32] C. Zhao and Y. Cai, "Trapping two types of particles using a focused partially coherent elegant Laguerre-Gaussian beam," *Opt. Lett.*, vol. 36, no. 12, pp. 2251–2253, Jun. 2011.
[33] Z. Liu and D. Zhao, "Radiation forces acting on a Rayleigh dielectric sphere produced by highly focused elegant Hermite-cosine-Gaussian beams," *Opt. Exp.*, vol. 20, no. 3, pp. 2895–2904, Jan. 2012.
[34] X. Liu and D. Zhao, "Optical trapping Rayleigh particles by using focused multi-Gaussian Schell-model beams," *Appl. Opt.*, vol. 53, no. 18, pp. 3976–3981, Jun. 2014.
[35] M. Luo and D. Zhao, "Simultaneous trapping of two types of particles by using a focused partially coherent cosine-Gaussian–correlated Schell-model beam," *Laser. Phys.*, vol. 24, no. 8, Jul. 2014, Art. no. 086001.
[36] X. Liu and D. Zhao, "Trapping two types of particles with a focused generalized multi-Gaussian Schell model beam," *Opt. Commun.*, vol. 354, pp. 250–255, Nov. 2015.
[37] F. Wang, X. Liu, Y. Yuan, and Y. Cai, "Experimental generation of partially coherent beams with different complex degrees of coherence," *Opt. Lett.*, vol. 38, no. 11, pp. 1814–1816, Jun. 2013.
[38] R. Chen, L. Liu, S. Zhu, G. Wu, F. Wang, and Y. Cai, "Statistical properties of a Laguerre-Gaussian Schell-model beam in turbulent atmosphere," *Opt. Exp.*, vol. 22, no. 2, pp. 1871–1883, Jan. 2014.
[39] L. Guo, Y. Chen, L. Liu, and Y. Cai, "Propagation of a Laguerre-Gaussian correlated Schell-model beam beyond the paraxial approximation," *Opt. Commun.*, vol. 352, pp. 127–134, Oct. 2015.
[40] J. Cang, P. Xiu, and X. Liu, "Propagation of Laguerre-Gaussian and Bessel-Gaussian Schell-model beams through paraxial optical systems in turbulent atmosphere," *Opt. Laser Technol.*, vol. 54, pp. 35–41, Dec. 2013.
[41] Y. Chen and Y. Cai, "Generation of a controllable optical cage by focusing a Laguerre-Gaussian correlated Schell-model beam," *Opt. Lett.*, vol. 39, no. 9, pp. 2549–2552, May 2015.
[42] Z. Zhu, L. Liu, F. Wang, and Y. Cai, "Evolution properties of a Laguerre-Gaussian correlated Schell-model beam propagating in uniaxial crystals orthogonal to the optical axis," *J. Opt. Soc. Amer. A*, vol. 32, no. 3, pp. 374–380, Mar. 2015.
[43] S. G. Reddy, A. Kumar, S. Prabhakar, and R. P. Singh, "Experimental generation of ring–shaped beams with random sources," *Opt. Lett.*, vol. 38, no. 21, pp. 4441–4444, Nov. 2013.
[44] Y. Chen, L. Liu, F. Wang, C. Zhao, and Y. Cai, "Elliptical Laguerre-Gaussian correlated Schell-model beam," *Opt. Exp.*, vol. 22, no. 11, pp. 13975–13987, Jun. 2014.
[45] Y. Chen, F. Wang, C. Zhao, and Y. Cai, "Experimental demonstration of a Laguerre-Gaussian correlated Schell-model vortex beam," *Opt. Exp.*, vol. 22, no. 5, pp. 5826–5838, Mar. 2014.
[46] H. F. Xu, Z. Zhang, J. Qu, and W. Huang, "The tight focusing properties of Laguerre-Gaussian–correlated Schell-model beams," *J. Mod. Optic.*, vol. 63, no. 15, pp. 1429–1437, Feb. 2016.
[47] Y. Cai and C. Chen, "Paraxial propagation of a partially coherent Hermite-Gaussian beam through aligned and misaligned ABCD optical systems," *J. Opt. Soc. Amer. A*, vol. 24, no. 8, pp. 2394–2401, Aug. 2007.
[48] H. F. Xu, W. J. Zhang, J. Qu, and W. Huang, "Optical trapping Rayleigh dielectric particles with focused partially coherent dark hollow beams," *J. Mod. Optic.*, vol. 62, no. 21, pp. 1839–1848, Jun. 2015.
[49] I. S. Gradshteyn and I. M. Ryzhik, *Table of Integrals, Series, and Products*. New York, NY, USA: Academic, 1994.
[50] I. Kimel and L. R. Elias, "Relations between Hermite and Laguerre Gaussian modes," *IEEE J. Quantum Electron.*, vol. 29, no. 9, pp. 2562–2567, Sep. 1993.
[51] Y. Zhang, T. Suyama, and B. Ding, "Longer axial trap distance and larger radial trap stiffness using a double–ring radially polarized beam," *Opt. Lett.*, vol. 35, no. 8, pp. 1281–1283, Apr. 2010.